

# Deuteron Magnetic Quadrupole Moment From Chiral Effective Field Theory

C.-P. Liu<sup>1</sup>, J. de Vries<sup>2</sup>, E. Mereghetti<sup>3</sup>,  
R. G. E. Timmermans<sup>2</sup>, and U. van Kolck<sup>4,5</sup>

<sup>1</sup> *Department of Physics, National Dong Hwa University,  
Shoufeng, Hualien 97401, Taiwan*

<sup>2</sup> *KVI, Theory Group, University of Groningen,  
9747 AA Groningen, The Netherlands*

<sup>3</sup> *Ernest Orlando Lawrence Berkeley National Laboratory,  
University of California, Berkeley, CA 94720, USA*

<sup>4</sup> *Institut de Physique Nucléaire, Université Paris-Sud, IN2P3/CNRS,  
F-91406 Orsay Cedex, France*

<sup>5</sup> *Department of Physics, University of Arizona,  
Tucson, AZ 85721, USA*

## Abstract

We calculate the magnetic quadrupole moment (MQM) of the deuteron at leading order in the systematic expansion provided by chiral effective field theory. We take into account parity ( $P$ ) and time-reversal ( $T$ ) violation which, at the quark-gluon level, results from the QCD vacuum angle and dimension-six operators that originate from physics beyond the Standard Model. We show that the deuteron MQM can be expressed in terms of five low-energy constants that appear in the  $P$ - and  $T$ -violating nuclear potential and electromagnetic current, four of which also contribute to the electric dipole moments of light nuclei. We conclude that the deuteron MQM has an enhanced sensitivity to the QCD vacuum angle and that its measurement would be complementary to the proposed measurements of light-nuclear EDMs.

Permanent electric dipole moments (EDMs) of particles, nuclei, atoms, and molecules are powerful probes for physics “beyond” the Standard Model (SM) of particle physics. EDMs violate both parity ( $P$ ) and time-reversal ( $T$ ) invariance (or, if we invoke the  $CPT$  theorem of relativistic quantum field theory,  $CP$  invariance). EDMs could be low-energy manifestations of some source of  $P$  and  $T$  violation ( $\cancel{PT}$ ) that originates at an energy scale comparable to or even higher than that accessed by the LHC. At the current experimental accuracy, electroweak quark mixing can be ignored, and the only Standard Model (SM) source that can impact EDMs is the QCD vacuum angle,  $\bar{\theta}$  [1]. A nonzero measurement of a hadronic EDM could be due to either beyond-the-SM  $\cancel{PT}$  sources or a finite value of  $\bar{\theta}$ , even though the current upper bound on the neutron EDM already limits this angle to a very small value. Among the possible beyond-the-SM  $\cancel{PT}$  sources, those represented by operators of effective dimension six [2] are expected to dominate: the quark EDM (qEDM), the quark and gluon chromo-electric dipole moments (qCEDM and gCEDM, respectively), and two independent four-quark (FQ) interactions. From a theoretical point of view, it is clearly an important priority to disentangle the dimension-four SM  $\bar{\theta}$ -term and the non-SM sources [3].

The deuteron is an excellent candidate for a sensitive EDM search in a storage ring [4]. In a recent paper [5] we addressed the EDMs of light nuclei, including the deuteron, within chiral effective field theory (EFT). The major advantage of such an EFT approach is its direct link to QCD in that it exploits the different chiral properties of the fundamental  $\cancel{PT}$  sources. Moreover, the power-counting scheme allows for a controlled framework such that the theoretical uncertainties can be estimated and the results can be improved systematically. We showed that the EDMs of light nuclei can be expressed in terms of essentially six  $\cancel{PT}$  parameters, or low-energy constants (LECs). These LECs can in principle be calculated from the underlying  $\cancel{PT}$  sources by solving QCD at low energies, in particular by lattice simulations. Lacking that, the size of the LECs can be estimated by naive dimensional analysis. We concluded that the EDMs of various light nuclei can give crucial complementary information about the fundamental  $\cancel{PT}$  sources.

Since it is a spin-1 particle, the deuteron has one other static  $\cancel{PT}$  electromagnetic moment, the magnetic quadrupole moment (MQM). In this paper, we address the deuteron MQM in the same framework that was used in Ref. [5]. It was shown in Ref. [3] that, in addition to LECs that contribute to the EDMs of light nuclei, the deuteron MQM depends also on  $\cancel{PT}$  pion-nucleon-photon interactions. Moreover, it was argued that only for the  $\bar{\theta}$  term is the deuteron MQM expected to be larger than the deuteron EDM (in appropriate units). For the beyond-the-SM sources, the MQM is expected to be of similar size or somewhat smaller than the EDM. This indicates that a measurement of the deuteron MQM, if possible, could play a central role in separating the various  $\cancel{PT}$  sources.

The conclusions of Ref. [3] were based on a chiral EFT in which the one-pion exchange nucleon-nucleon ( $NN$ ) force is treated in perturbation theory [6]. This approach, expected to be valid at low energies, allows one to give analytical results for the deuteron EDM and MQM, which, moreover, can be extended to sub-leading orders. On the other hand, in  $NN$  scattering it was found that the results do not converge in certain partial waves for momenta somewhat lower than expected [7]. It is therefore important to check the

results of Ref. [3] in the framework of a chiral EFT that treats pions nonperturbatively [8]. For the deuteron EDM it was found that the two EFTs gave similar results [5]. In this article we investigate this for the deuteron MQM as well and we address the question, to what extent a possible measurement of the MQM could be of help to separate the different  $\mathcal{PT}$  sources. We also compare our results to previous studies of the deuteron MQM [9, 10]. In particular, Ref. [10] used traditional meson-exchange  $NN$  models and a general  $\mathcal{PT}$   $NN$  interaction [10, 11]. We use the codes of Ref. [10], but adapt and extend the framework (the  $\mathcal{PT}$   $NN$  potentials and currents) to chiral EFT with nonperturbative pions. We follow the hybrid approach of Ref. [5] in which nonperturbative pion exchange is embedded into the  $P$ - and  $T$ -conserving ( $PT$ ) wave functions of modern, “realistic” potentials [12, 13]. In principle our framework can be applied to the calculation of the MQM of other light nuclei as well.

We start our discussion of the deuteron MQM from the effective hadronic Lagrangian involving the low-energy degrees of freedom: nucleon ( $N$ ), photon ( $A_\mu$ ), and pion ( $\pi$ ). The  $PT$  part, which originates from the quark kinetic (color- and electromagnetically gauged) and mass terms in QCD, is well-known [14, 5]. At leading order (LO) it consists of the standard pion-nucleon axial-vector coupling,  $g_A = 1.27$ , and the pion-nucleon-photon interaction obtained from gauging the  $g_A$  term. The pion-photon interactions stem from the pion charge. At next-to-leading order (NLO), the photon couples to the nucleon via the covariant derivative in the nucleon kinetic term and via the isoscalar and isovector magnetic moments, respectively  $\kappa_0 = -0.12$  and  $\kappa_1 = 3.7$ . The  $\mathcal{PT}$  effective Lagrangian results from the most general  $\mathcal{PT}$  Lagrangian at the quark-gluon level. It was derived and discussed in detail in Refs. [15, 16]. The key observation is that the different fundamental  $\mathcal{PT}$  sources transform differently under chiral symmetry and therefore generate different hadronic interactions. Given enough independent observables it will be possible to disentangle them [3].

We present here only the terms that are relevant for the LO MQM calculation, which depends on five  $\mathcal{PT}$  interactions. The Lagrangian

$$\begin{aligned} \mathcal{L}_{\mathcal{PT}} = & -\frac{1}{F_\pi} \bar{N} (\bar{g}_0 \boldsymbol{\tau} \cdot \boldsymbol{\pi} + \bar{g}_1 \pi_3) N + \frac{\bar{c}_\pi}{F_\pi} \epsilon^{\mu\nu\alpha\beta} v_\alpha \bar{N} S_\beta \boldsymbol{\tau} \cdot \boldsymbol{\pi} N F_{\mu\nu} \\ & + \bar{C}_1 \bar{N} N \partial_\mu (\bar{N} S^\mu N) + \bar{C}_2 \bar{N} \boldsymbol{\tau} N \cdot \mathcal{D}_\mu (\bar{N} S^\mu \boldsymbol{\tau} N) , \end{aligned} \quad (1)$$

contains isoscalar ( $\bar{g}_0$ ) and isovector ( $\bar{g}_1$ ) nonderivative pion-nucleon couplings, an isoscalar pion-nucleon-photon coupling ( $\bar{c}_\pi$ ), and two short-range  $\mathcal{PT}$   $NN$  interactions ( $\bar{C}_1$ ,  $\bar{C}_2$ ). Here  $F_\pi = 185$  MeV is the pion decay constant,  $\boldsymbol{\tau}$  are the Pauli matrices in isospin space,  $v_\mu$  ( $S_\mu$ ) is the nucleon velocity (spin),  $\epsilon^{\mu\nu\alpha\beta}$  (with  $\epsilon^{0123} = 1$ ) the completely antisymmetric tensor,  $F_{\mu\nu} = \partial_\mu A_\nu - \partial_\nu A_\mu$  the photon field strength, and  $(\mathcal{D}_\mu)_{ab} = \delta_{ab} \partial_\mu + e \epsilon_{3ab} A_\mu + \mathcal{O}(\boldsymbol{\pi} \cdot \partial_\mu \boldsymbol{\pi} / F_\pi^2)$  a chiral covariant derivative. Except for  $\bar{c}_\pi$ , these interactions play a role in the calculation of nuclear EDMs [3, 5, 17] as well. The scaling of the LECs in terms of the pion mass ( $m_\pi$ ), the characteristic QCD scale ( $M_{\text{QCD}} \sim 2\pi F_\pi$ ), and the scale of  $\mathcal{PT}$  physics beyond the SM is given in Ref. [5] for  $\bar{g}_0$ ,  $\bar{g}_1$ ,  $\bar{C}_1$ , and  $\bar{C}_2$ . The pion-nucleon-photon coupling  $\bar{c}_\pi$  has the same scaling as the short-range contribution to the isoscalar nucleon EDM,  $\bar{d}_0$  [3].

The calculation of the deuteron MQM can be divided into two contributions. The first contribution comes from an insertion of the  $\cancel{PT}$  electromagnetic two-body current  $\vec{J}_{\cancel{PT}}$ . The current has to be two-body since the constituent nucleons, being spin-1/2 particles, do not possess a MQM. The second contribution comes from the electromagnetic current  $\vec{J}_{PT}$  upon perturbing the wave function of the nucleus with the  $\cancel{PT}$  potential  $V_{\cancel{PT}}$ , such that the wave function obtains a  $\cancel{PT}$  component. This current can be one- or two-body. The required  $\cancel{PT}$  potential  $V_{\cancel{PT}}$  and current  $\vec{J}_{\cancel{PT}}$  can be calculated from Eq. (1).

To first order in the  $\cancel{PT}$  sources, the deuteron MQM is thus a sum of two reduced matrix elements,

$$\mathcal{M}_d = \frac{1}{\sqrt{30}} \left( \langle \Psi_d | \widetilde{\mathbf{M}} | \Psi_d \rangle + 2 \langle \Psi_d | \mathbf{M} | \widetilde{\Psi}_d \rangle \right). \quad (2)$$

The deuteron ground state  $|\Psi_d\rangle$  and its parity admixture  $|\widetilde{\Psi}_d\rangle$  are the solutions of homogeneous and inhomogeneous Schrödinger equations,

$$(E - H_{PT})|\Psi_d\rangle = 0, \quad (3)$$

$$(E - H_{PT})|\widetilde{\Psi}_d\rangle = V_{\cancel{PT}}|\Psi_d\rangle, \quad (4)$$

respectively, where  $H_{PT}$  is the  $PT$  Hamiltonian. The MQM operators  $\mathbf{M}$  and  $\widetilde{\mathbf{M}}$  are obtained from the corresponding currents  $\vec{J}_{PT}$  and  $\vec{J}_{\cancel{PT}}$ , respectively. The Cartesian component along the  $z$  direction,  $M_{33}$ , which is proportional to the spherical harmonic  $Y_2^0$ , takes the form

$$M_{33} = 2 \int d^3x x_3 (\vec{x} \times \vec{J}(\vec{x}))_3, \quad (5)$$

where  $\vec{x}$  is the position where the current density is probed. Given the current in momentum space,

$$\vec{J}(\vec{q}) = \int d^3x e^{-i\vec{q}\cdot\vec{x}} \vec{J}(\vec{x}), \quad (6)$$

$M_{33}$  can also be derived as

$$M_{33} = -2 \lim_{\vec{q} \rightarrow 0} (\nabla_{q_3} \nabla_{q_1} J_2(\vec{q}) - \nabla_{q_3} \nabla_{q_2} J_1(\vec{q})). \quad (7)$$

The three classes of contributions to the deuteron MQM described above are shown in Fig. 1. In order to decide which diagrams give the main contribution to the MQM we apply the power counting rules outlined in Ref. [5]. These rules provide an expansion in  $Q/M_{\text{QCD}}$ , where  $Q$  is the generic momentum in the process, in this case of the order of the deuteron binding momentum. We use  $Q \sim m_\pi \sim F_\pi$ , as standard in  $\chi$ PT. For each class we take the  $PT$  vertices from the interactions described above and the  $\cancel{PT}$  LO vertices from Eq. (1). The iteration of the LO  $PT$  potential is not suppressed, and is necessary among nucleons in reducible intermediate states, as indicated in diagrams (b) and (c) of Fig. 1. Such iteration among nucleons before and after any  $\cancel{PT}$  insertion builds up the  $PT$  wave function, represented in Fig. 1 by the triangles. In the following power counting

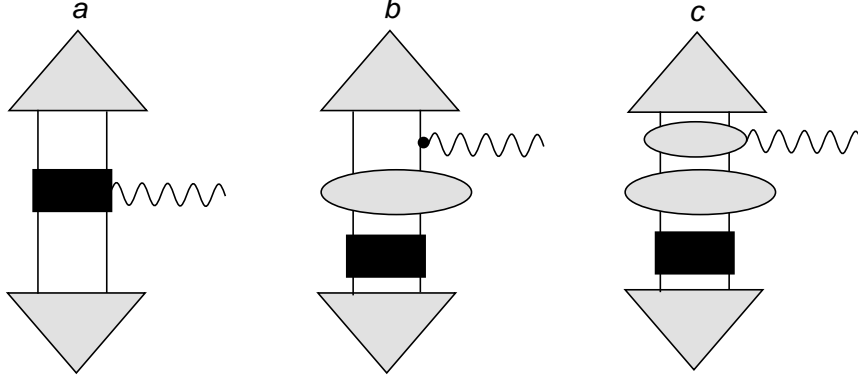


Figure 1: The three general classes of diagrams contributing to the deuteron MQM described in the text. Solid and wavy lines represent nucleons and photons. The large triangle denotes the  $PT$  wave function and the oval iterations of the  $PT$  potential. The nucleon-photon vertex is the nucleon magnetic moment or the convection current, and the photon attached to the oval is the  $PT$  two-body current. The black squares without (with) an attached photon represent the  $\cancel{PT}$  potential (two-body current).

we omit this overall factor. The scaling in terms of the LECs in Eq. (1) of diagram (a) is then

$$D_a = \mathcal{O}\left(e \frac{\bar{g}_0}{F_\pi^2} \frac{Q^2}{M_{\text{QCD}}}\right) + \mathcal{O}\left(\frac{\bar{c}_\pi Q^2}{F_\pi^2} \frac{Q^2}{M_{\text{QCD}}}\right) + \mathcal{O}\left(e \bar{C}_2 F_\pi^2 \frac{Q^2}{M_{\text{QCD}}}\right), \quad (8)$$

while diagrams (b) and (c) scale as

$$D_{b,c} = \mathcal{O}\left(e \frac{\bar{g}_{0,1}}{F_\pi^2} \frac{Q^2}{M_{\text{QCD}}}\right) + \mathcal{O}\left(e \bar{C}_{1,2} F_\pi^2 \frac{Q^2}{M_{\text{QCD}}}\right). \quad (9)$$

Which contribution dominates depends on the fundamental  $\cancel{PT}$  source, the dimension-four  $\bar{\theta}$ -term and the dimension-six terms: qEDM, qCEDM, gCEDM, and FQ.

- For the  $\bar{\theta}$  term, only the isoscalar coupling  $\bar{g}_0$  plays a role at LO. In order to generate  $\bar{g}_1$ , the  $\bar{\theta}$  term requires an insertion of the quark mass difference, which causes a relative suppression of  $\bar{g}_1$  relative to  $\bar{g}_0$  by a factor  $\varepsilon m_\pi^2/M_{\text{QCD}}^2$  [15], where  $\varepsilon = (m_d - m_u)/(m_u + m_d)$ . The other couplings,  $\bar{c}_\pi$  and  $\bar{C}_{1,2}$ , also contribute at sub-leading orders. Since  $\bar{g}_0$  enters in principle through the three classes of diagrams with similar factors, all these classes are equally important.
- For the qCEDM, we need both pion-nucleon interactions, since there is no relative suppression of  $\bar{g}_1$ . Again, all three classes are, a priori, equally important.
- For the qEDM, the purely hadronic interactions are suppressed by factors of the fine-structure constant, and only  $\bar{c}_\pi$  is important. Thus only diagram (a) matters.
- For the chiral-invariant ( $\chi$ I)  $\cancel{PT}$  sources (gCEDM and FQ), the pion-nucleon interactions, which break chiral symmetry, are suppressed by a factor  $m_\pi^2/M_{\text{QCD}}^2$  compared

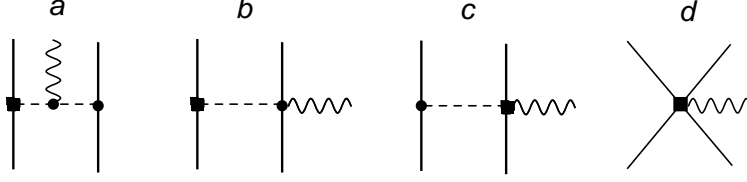


Figure 2: Diagrams contributing to the  $\mathcal{PT}$  two-nucleon current. Solid, dashed, and wavy lines represent nucleons, pions, and photons. A square marks a  $\mathcal{PT}$  interaction and the other vertices  $PT$  interactions. Only one topology per diagram is shown.

to the  $\mathcal{PT}$  short-range  $NN$  interactions, which conserve chiral symmetry. The latter are therefore as important as the pion-nucleon interactions. For the  $\chi$ I sources again all three diagrams could be important.

We now turn to the calculation of the various ingredients in these diagrams, starting with the currents. For the nucleons we use incoming momenta  $\vec{p}_1 = \vec{P}/2 + \vec{p}$  and  $\vec{p}_2 = \vec{P}/2 - \vec{p}$ , and outgoing momenta  $\vec{p}'_1 = \vec{P}'/2 + \vec{p}'$  and  $\vec{p}'_2 = \vec{P}'/2 - \vec{p}'$ . The photon momentum  $\vec{q} = \vec{P} - \vec{P}'$  is outgoing. For convenience we introduce  $\vec{k} = \vec{p} - \vec{p}'$ . The spin (isospin) of nucleon  $i$  is denoted by  $\vec{\sigma}^{(i)}/2$  ( $\vec{\tau}^{(i)}/2$ ).

The relevant  $\mathcal{PT}$  two-body currents that appear in diagram class (a) of Fig. 1 are shown in Fig. 2. Since the deuteron wave function is isoscalar, the  $\mathcal{PT}$  currents need to be isoscalar as well in order to contribute to the MQM. Only the current in diagram (c), which stems from qEDM, meets this requirement, and we find

$$\vec{J}_{\mathcal{PT}}(\vec{q}, \vec{k}) = -\frac{g_A \bar{c}_\pi}{F_\pi^2} \vec{\tau}^{(1)} \cdot \vec{\tau}^{(2)} \left[ \vec{\sigma}^{(1)} \times \vec{q} \frac{\vec{\sigma}^{(2)} \cdot (\vec{k} - \vec{q}/2)}{(\vec{k} - \vec{q}/2)^2 + m_\pi^2} - \vec{\sigma}^{(2)} \times \vec{q} \frac{\vec{\sigma}^{(1)} \cdot (\vec{k} + \vec{q}/2)}{(\vec{k} + \vec{q}/2)^2 + m_\pi^2} \right]. \quad (10)$$

In diagram classes (b) and (c) of Fig. 1 the photon interacts instead with a  $PT$  current. The  $PT$  one-body current in diagram (b) is either the nucleon magnetic moment or the convection current coming from the nucleon kinetic energy,

$$\vec{J}_{PT}(\vec{q}, \vec{p}_i) = \frac{e}{4m_N} \left\{ \left[ 1 + \kappa_0 + (1 + \kappa_1) \tau_3^{(i)} \right] i \vec{\sigma}^{(i)} \times \vec{q} + \left( 1 + \tau_3^{(i)} \right) (2\vec{p}_i - \vec{q}) \right\}, \quad (11)$$

where  $i$  is the index of the nucleon that interacts with the photon. In diagram (c) we require the  $PT$  two-body currents depicted in Fig. 3:

$$\begin{aligned} \vec{J}_{PT}(\vec{q}, \vec{k}) = & i \frac{e g_A^2}{F_\pi^2} (\vec{\tau}^{(1)} \times \vec{\tau}^{(2)})_3 \left\{ -2\vec{k} \frac{\vec{\sigma}^{(1)} \cdot (\vec{k} + \vec{q}/2)}{(\vec{k} + \vec{q}/2)^2 + m_\pi^2} \frac{\vec{\sigma}^{(2)} \cdot (\vec{k} - \vec{q}/2)}{(\vec{k} - \vec{q}/2)^2 + m_\pi^2} \right. \\ & \left. + \vec{\sigma}^{(1)} \frac{\vec{\sigma}^{(2)} \cdot (\vec{k} - \vec{q}/2)}{(\vec{k} - \vec{q}/2)^2 + m_\pi^2} + \vec{\sigma}^{(2)} \frac{\vec{\sigma}^{(1)} \cdot (\vec{k} + \vec{q}/2)}{(\vec{k} + \vec{q}/2)^2 + m_\pi^2} \right\}. \end{aligned} \quad (12)$$

With the methods outlined in Refs. [18, 5], these currents can straightforwardly be Fourier transformed to coordinate space, where we denote by  $\vec{x}^{(i)}$  the position of nucleon

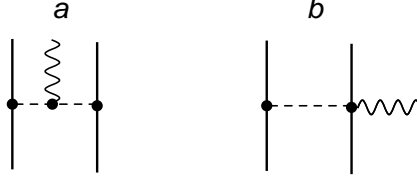


Figure 3: Diagrams contributing to the  $PT$  two-nucleon current.

$i$  and by  $\vec{r} = \vec{x}^{(1)} - \vec{x}^{(2)}$  the relative position. We also introduce the Yukawa function

$$U(r) = \frac{e^{-m_\pi r}}{4\pi r}. \quad (13)$$

The MQM operators are, from Eq. (10),

$$\begin{aligned} \widetilde{M}_{33} = & 2 \frac{g_A \bar{C}_\pi}{F_\pi^2} \boldsymbol{\tau}^{(1)} \cdot \boldsymbol{\tau}^{(2)} \left[ \left( 3 \sigma_3^{(1)} x_3^{(1)} - \vec{\sigma}^{(1)} \cdot \vec{x}^{(1)} \right) \vec{\sigma}^{(2)} \right. \\ & \left. - \left( 3 \sigma_3^{(2)} x_3^{(2)} - \vec{\sigma}^{(2)} \cdot \vec{x}^{(2)} \right) \vec{\sigma}^{(1)} \right] \cdot \vec{\nabla}_r U(r), \end{aligned} \quad (14)$$

and from Eqs. (11) and (12),

$$\begin{aligned} M_{33} = & \frac{e}{2m_N} \left\{ \left[ 1 + \kappa_0 + (1 + \kappa_1) \tau_3^{(i)} \right] \left( 3 \sigma_3^{(i)} x_3^{(i)} - \vec{\sigma}^{(i)} \cdot \vec{x}^{(i)} \right) \right. \\ & \left. + 2 \left( 1 + \tau_3^{(i)} \right) \vec{x}_3^{(i)} (\vec{x}^{(i)} \times \vec{p}^{(i)})_3 \right\} \\ & - \frac{e g_A^2}{2 F_\pi^2} (\boldsymbol{\tau}^{(1)} \times \boldsymbol{\tau}^{(2)})_3 \left\{ \left[ \sigma_3^{(1)} (\vec{\sigma}^{(2)} \times \vec{r})_3 + \sigma_3^{(2)} (\vec{\sigma}^{(1)} \times \vec{r})_3 \right] \right. \\ & \left. + 4 \left[ x_3^{(1)} (\vec{x}^{(1)} \times \vec{\sigma}^{(1)})_3 \vec{\sigma}^{(2)} + x_3^{(2)} (\vec{x}^{(2)} \times \vec{\sigma}^{(2)})_3 \vec{\sigma}^{(1)} \right] \cdot \vec{\nabla}_r \right\} U(r), \end{aligned} \quad (15)$$

where  $\vec{p}^{(i)} = -i \vec{\nabla}_{x^{(i)}}$ .

The last ingredients we need are the deuteron wave function  $\Psi_d$  and its parity admixture  $\tilde{\Psi}_d$ . They have been calculated in Ref. [10] using modern high-quality phenomenological  $PT$  potentials and a  $PT$  potential dominated by pion exchange and extended with heavy-meson exchange. In the EFT spirit, it would be best to calculate  $\Psi_d$  from a  $PT$  Hamiltonian fully consistent with chiral symmetry and renormalization-group invariance, but an accurate fit to two-nucleon data with these properties does not yet exist. For those sources for which the MQM is dominated by long-distance physics, we expect no significant differences when using the phenomenological potentials, and thus for  $\Psi_d$  we use the results of Ref. [10]. For comparison with Ref. [5], we give below numbers corresponding to the Argonne  $v_{18}$  (AV18) potential [12]. Differences with results obtained from the NijmII and Reid93 potentials [13] are within a few percent, except for the cases of  $\bar{C}_{1,2}$  insertion—for which more details will be provided later.

The ground state of the deuteron is mainly a  $^3S_1$  state with some  $^3D_1$  admixture. The matrix element of  $\widetilde{\mathbf{M}}$  is found to be

$$\frac{1}{\sqrt{30}} \langle \Psi_d | \widetilde{\mathbf{M}} | \Psi_d \rangle = 0.07 \frac{F_\pi \bar{C}_\pi}{e} e \text{ fm}^2. \quad (16)$$

The relevant matrix elements of  $\mathbf{M}$  are obtained with  $\tilde{\Psi}_d$  from the LO  $\cancel{PT}$  two-nucleon potential. The general  $\cancel{PT}$   $NN$  potential was derived in Ref. [19] and we summarize the relevant parts here. In coordinate space the potential is given by

$$\begin{aligned} V_{\cancel{PT}}(\vec{r}) = & -\frac{\bar{g}_0 g_A}{F_\pi^2} \boldsymbol{\tau}^{(1)} \cdot \boldsymbol{\tau}^{(2)} (\vec{\sigma}^{(1)} - \vec{\sigma}^{(2)}) \cdot (\vec{\nabla}_r U(r)) \\ & -\frac{\bar{g}_1 g_A}{2F_\pi^2} \left[ (\tau_3^{(1)} + \tau_3^{(2)}) (\vec{\sigma}^{(1)} - \vec{\sigma}^{(2)}) + (\tau_3^{(1)} - \tau_3^{(2)}) (\vec{\sigma}^{(1)} + \vec{\sigma}^{(2)}) \right] \cdot (\vec{\nabla}_r U(r)) \\ & +\frac{1}{2} [\bar{C}_1 + \bar{C}_2 \boldsymbol{\tau}^{(1)} \cdot \boldsymbol{\tau}^{(2)}] (\vec{\sigma}^{(1)} - \vec{\sigma}^{(2)}) \cdot (\vec{\nabla}_r \delta^{(3)}(\vec{r})). \end{aligned} \quad (17)$$

In this expression, at LO  $\bar{g}_0$  originates from  $\bar{\theta}$  term, qCEDM, and  $\chi$ I sources;  $\bar{g}_1$  from qCEDM and  $\chi$ I sources; and  $\bar{C}_i$  from  $\chi$ I sources only.

If the parity admixture comes from a  $\bar{g}_1$  pion exchange, the deuteron wave function acquires a  $^3P_1$  component. In order to get back to the ground state, the deuteron can couple to the photon via the isovector one-body or the two-body currents in Eqs. (11) and (12), respectively. The result is

$$\frac{2}{\sqrt{30}} \langle \Psi_d | | \mathbf{M} | | \tilde{\Psi}_d(^3P_1) \rangle = - \left[ 0.031(1 + \kappa_1) + 0.003 + 0.008 \right] \frac{\bar{g}_1}{F_\pi} e \text{ fm}^2, \quad (18)$$

where the first and second terms come from the isovector magnetic moment due to the spin and convection current, respectively; and the third term from the  $PT$  two-body current.

After a  $\bar{g}_0$  pion exchange or an insertion of  $\bar{C}_{1,2}$  the deuteron wave function obtains a  $^1P_1$  component instead. In this case, the deuteron needs to couple to the isoscalar nucleon magnetic moment or an isoscalar two-body current, which is not present at LO. The result is

$$\frac{2}{\sqrt{30}} \langle \Psi_d | | \mathbf{M} | | \tilde{\Psi}_d(^1P_1) \rangle = - \left[ 0.044 \frac{\bar{g}_0}{F_\pi} + 0.0013 F_\pi^3 (\bar{C}_1 - 3\bar{C}_2) \right] (1 + \kappa_0) e \text{ fm}^2. \quad (19)$$

For the contact interaction with

$$\bar{C}_0 \equiv \bar{C}_1 - 3\bar{C}_2 \quad (20)$$

we apply a strategy followed in Refs. [20, 5]: it is simulated in our calculations by a fictitious heavy-meson (of mass  $m$ ) exchange, since

$$\frac{m^2 \bar{C}_0}{4\pi r} e^{-mr} \rightarrow \bar{C}_0 \delta^{(3)}(\vec{r}) \quad (21)$$

as  $m$  goes to infinity. As shown in Fig. 4, when  $m$  reaches 2.5 GeV, the results converge at about  $\lesssim 10\%$  level, so we report the above numbers at this scale. While in this figure one sees good consistency between the AV18 and NijmII results, the Reid93 result is off by a factor of 2. The main reason is that the Reid93 potential generates a deuteron  $S$  state whose short-distance wave function is enhanced, leading to more sensitivity to  $\bar{C}_0$ .



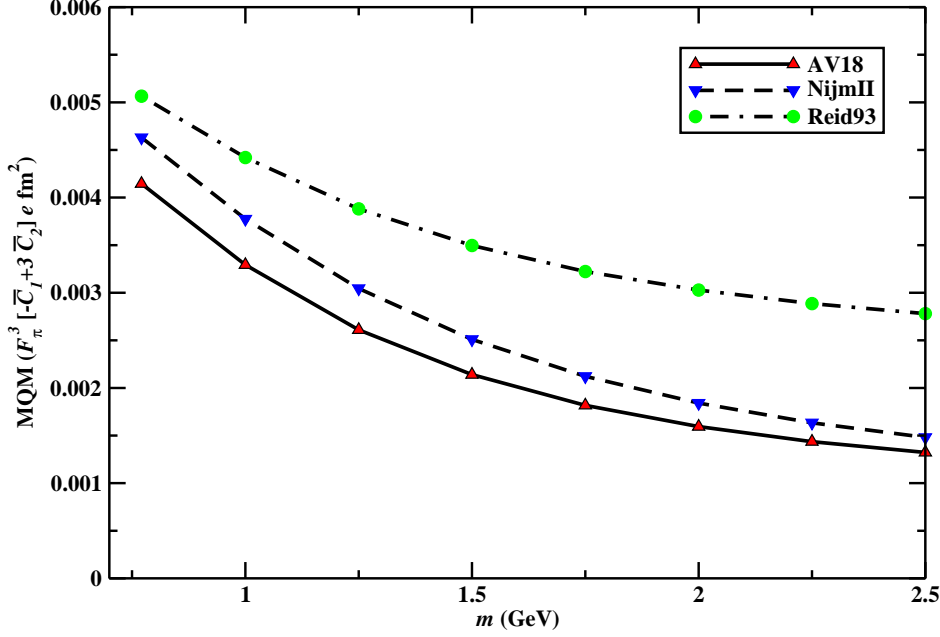


Figure 4: Deuteron MQM due to the  $F_\pi^3(-\bar{C}_1+3\bar{C}_2)$  short-range  $\mathcal{PT}$  interaction as function of a regulating mass  $m$ , for various  $PT$  Hamiltonians.

The large discrepancy between different potentials suggests that for  $\chi$ I sources, for which  $\bar{C}_0$  contributes to the MQM at leading order, a fully consistent calculation of  $\Psi_d$  within EFT is necessary if this part of the matrix element needs to be known better than within a factor of 2.

The dependence of the deuteron MQM on  $\bar{g}_{0,1}$ ,  $\bar{C}_0$ , and  $\bar{c}_\pi$  was studied in Ref. [3] in a framework where pion exchange is treated perturbatively. At LO in that framework, the coefficients in front of  $\bar{g}_0(1+\kappa_0)/F_\pi$  and  $\bar{g}_1(1+\kappa_1)/F_\pi$  were found to be, respectively,  $-0.146$  and  $-0.049$ , in agreement with the results in Ref. [9] where a zero-range approximation for the  $NN$  interaction was assumed. Considering the large intrinsic uncertainty ( $\sim 30\%$ ) in the perturbative-pion calculation, the perturbative-pion  $\bar{g}_1$  coefficient is in reasonable agreement with Eq. (18). A similar agreement was found for the deuteron EDM [5]. On the other hand, the perturbative-pion  $\bar{g}_0$  coefficient is three times larger than Eq. (19), suggesting that the effects of additional pion exchanges, neglected in the LO perturbative calculation, are larger in the  $^1P_1$  channel than in the  $^3P_1$  channel. We have verified that, if the tensor force is ignored and the same strong force is assumed for both the  $^1P_1$  and  $^3P_1$  channels, the ratio of the strong parts of the MQM matrix elements due to the isoscalar and isovector one-body currents becomes 3, which is consistent with

Refs. [9, 3]. Preliminary results of an NLO calculation in the perturbative-pion framework indicate that, indeed, NLO corrections influence the  $\bar{g}_0$  coefficient by a larger amount than the  $\bar{g}_1$  coefficient [21].

In the framework of perturbative pions, the  $PT$  convection and two-body currents in diagram (b) and (c) of Fig. 1 enter at NLO and are expected to be smaller than the contribution from the isovector magnetic moment. This agrees with the numerical results in Eq. (18) where the convection and two-body currents only enter at the  $\sim 5\%$  level. These currents would have been small ( $\sim 30\%$ ) even if the isovector magnetic moment had been more natural, that is, if  $1 + \kappa_1$  were  $\simeq 1$ .

The result for  $\bar{c}_\pi$  in Eq. (16) is somewhat smaller than expected from the power counting estimate in Eq. (8),  $\mathcal{M}_d(\text{qEDM}) \sim 0.2F_\pi\bar{c}_\pi\text{fm}^2$ , and is more in line with the expectation of the perturbative-pion calculation,  $\mathcal{O}(\gamma\bar{c}_\pi/M_{NN}M_{\text{QCD}}) \sim 0.07F_\pi\bar{c}_\pi\text{fm}^2$ , where  $M_{NN} = 4\pi F_\pi^2/g_A^2 m_N$  is the characteristic scale where pions become nonperturbative [6] and  $\gamma$  the deuteron binding momentum. A more detailed comparison with the perturbative-pion calculation is complicated by the appearance of a short-range current, which is needed for renormalization purposes. Neglecting the counterterm and using for the renormalization scale  $\mu = M_{NN}$ , the perturbative result becomes  $0.08F_\pi\bar{c}_\pi\text{fm}^2$ , in good agreement with Eq. (16). A comparison between the contributions from the short-range  $\cancel{PT}$   $NN$  interactions in the perturbative and nonperturbative calculations is not useful because the LEC  $\bar{C}_0$  includes different physics and thus has different scalings in the two EFTs.

The deuteron MQM was previously calculated in Refs. [9, 10], in which the deuteron MQM was assumed to be dominated by  $\cancel{PT}$  one-pion exchange (OPE). Since these calculations did not use the chiral properties of the fundamental  $\cancel{PT}$  sources, the  $\cancel{PT}$  pion-nucleon interactions were assumed to be all of the same size. Our analysis shows that these assumptions only hold in case of a qCEDM. For  $\bar{g}_0$  and  $\bar{g}_1$  OPE we confirm the results in Ref. [10], but our  $\bar{g}_0$  result is 3 times smaller than the result in Ref. [9] due the discrepancy discussed above.

We are now in the position to discuss the results for the various  $\cancel{PT}$  sources. It was noted in Ref. [3] that the observation of a deuteron MQM, together with the nucleon and deuteron EDMs, could provide important clues to separate the various  $\cancel{PT}$  sources. In particular, it was concluded that only for chiral-symmetry-breaking, but isoscalar, sources like the QCD  $\bar{\theta}$  term is the deuteron MQM, in appropriate units, substantially larger than the deuteron EDM. For chiral- and isospin-breaking sources, like the qCEDM, the deuteron MQM and EDM are expected to be of the same size, and a measurement of both would fix the couplings  $\bar{g}_0$  and  $\bar{g}_1$ , allowing a prediction of other  $\cancel{PT}$  observables, like the  $^3\text{He}$  EDM. For the  $\chi\text{I}$  sources and the qEDM, in the perturbative-pion approach the MQM depends on one- and two-body LECs that do not contribute to the EDM. For these sources the MQM was found to be of the same size, or slightly smaller, than the EDM, but an observation of the MQM would not give us predictive power. These conclusions, based on the perturbative-pion power counting, are confirmed here by the nonperturbative results.

For the QCD  $\bar{\theta}$  term, the deuteron EDM is dominated by the isoscalar nucleon EDM,

$d_d \sim 2\bar{d}_0$  [3, 5]. A naturalness lower bound on the isoscalar nucleon EDM is provided by the non-analytic terms stemming from the pion cloud [22],  $|\bar{d}_0| \gtrsim 0.01(|\bar{g}_0|/F_\pi) e \text{ fm}$ . The deuteron MQM is dominated by the  $\bar{g}_0$  piece in Eq. (19). Combining the two with the deuteron mass  $m_d$ , we find

$$\left| \frac{m_d \mathcal{M}_d}{d_d} \right| \simeq 0.21(1 + \kappa_0) \left| \frac{\bar{g}_0}{F_\pi \bar{d}_0} \right| e \text{ fm} \lesssim 21(1 + \kappa_0). \quad (22)$$

At LO in the perturbative-pion approach, this ratio is about three times larger, as discussed above. Nonetheless, the nonperturbative calculation confirms that for isoscalar chiral-breaking sources the deuteron MQM is expected to be larger than the EDM in units of  $m_d$ .

In case of the qCEDM, where  $\bar{g}_0$  and  $\bar{g}_1$  have similar scalings, both the deuteron EDM and MQM are dominated by pion exchange. At LO, the EDM depends on  $\bar{g}_1$  only [5], and the MQM on the  $\bar{g}_{0,1}$  contributions in Eqs. (18) and (19). The MQM/EDM ratio becomes

$$\frac{m_d \mathcal{M}_d}{d_d} \simeq 1.6(1 + \kappa_1) + 2.2(1 + \kappa_0) \frac{\bar{g}_0}{\bar{g}_1} + 0.6, \quad (23)$$

which formally is  $\mathcal{O}(1)$ . However, due to the large anomalous isovector magnetic moment, numerically the ratio could be  $\mathcal{O}(10)$ . This means that the measurement of a large MQM/EDM ratio does not necessarily imply that the  $\bar{\theta}$  term is the dominant  $\mathcal{PT}$  mechanism.

If a qEDM is the dominant  $\mathcal{PT}$  source, the MQM is given by Eq. (16). It is solely coming from a two-body  $\mathcal{PT}$  current. The EDM is given by the sum of the neutron and the proton EDM,  $d_d \simeq 2\bar{d}_0$  [5]. Combining these results gives

$$\frac{m_d \mathcal{M}_d}{d_d} \simeq 0.7 \frac{\bar{c}_\pi}{\bar{d}_0}, \quad (24)$$

which is  $\mathcal{O}(1)$  by naive dimensional analysis (NDA). As we observed in the previous discussion, the matrix element of the operator with coefficient  $\bar{c}_\pi$  is smaller than the power counting estimate, so a more accurate conclusion is that, for  $\mathcal{PT}$  from the qEDM, the deuteron MQM is expected to be slightly smaller than the EDM, in agreement with Ref. [3].

Finally, for chiral-invariant sources, the MQM is dominated by the sum of Eqs. (18) and (19). From the NDA estimates in Ref. [5], we find  $F_\pi^4 \bar{C}_0 / \bar{g}_0 = \mathcal{O}(F_\pi^2 / m_\pi^2) \simeq 2$ , such that the  $\bar{C}_0$  contribution only enters at the  $\sim 10\%$  level. The deuteron EDM at LO formally depends on  $\bar{g}_1$  and the isoscalar nucleon EDM, but numerically the latter is expected to dominate, with pion-exchange corrections at the  $\sim 15\%$  level [5]. Ignoring the numerically small convection and two-body currents,

$$\left| \frac{m_d \mathcal{M}_d}{d_d} \right| \simeq \left[ 0.21(1 + \kappa_0) \left| \frac{\bar{g}_0}{F_\pi \bar{d}_0} \right| + 0.15(1 + \kappa_1) \left| \frac{\bar{g}_1}{F_\pi \bar{d}_0} \right| \right] e \text{ fm}. \quad (25)$$

By power counting we would expect the ratio to be  $\mathcal{O}(1)$ , but since the deuteron is weakly bound, pion exchange is smaller than expected. Using the NDA estimate  $|\bar{d}_0| \sim 5(|\bar{g}_{0,1}|/F_\pi) \text{ e fm}$ , we conclude that for  $\chi\text{I}$  sources the deuteron MQM should be smaller than the EDM.

In conclusion, we computed the deuteron MQM for various  $\mathcal{PT}$  sources: the QCD  $\bar{\theta}$  term, quark EDM, quark and gluon chromo-EDMs, and chiral-invariant four-quark operators. We performed these computations at leading order in the framework of chiral EFT, with pions treated nonperturbatively. The same parameters as in the corresponding calculation of light-nuclear EDMs appeared here, except for the quark EDM, which involves an independent short-range two-nucleon current. While the results confirm the qualitative conclusions of Ref. [3], there are important quantitative differences. Due to its enhanced sensitivity to the QCD  $\bar{\theta}$  term, a potential measurement of the deuteron MQM would be complementary to one of the deuteron EDM.

**Acknowledgments.** We thank G. Onderwater for helpful discussions. UvK is grateful to KVI for hospitality. This research was supported by the ROC NSC under grant NSC98-2112-M-259-004-MY3 (CPL), by the Dutch Stichting FOM under programs 104 and 114 (JdV, RGET), and by the US DOE under contract DE-AC02-05CH11231 with the Director, Office of Science, Office of High Energy Physics (EM), and under grants DE-FG02-06ER41449 (EM) and DE-FG02-04ER41338 (EM, UvK).

## References

- [1] G. 't Hooft, Phys. Rev. Lett. **37**, 8 (1976); C. G. Callan Jr., R. F. Dashen, and D. J. Gross, Phys. Lett. B **63**, 334 (1976); R. Jackiw and C. Rebbi, Phys. Rev. Lett. **37**, 172 (1976).
- [2] W. Buchmüller and D. Wyler, Nucl. Phys. B **268**, 621 (1986); A. De Rújula, M. B. Gavela, O. Pène, and F. J. Vegas, Nucl. Phys. B **357**, 311 (1991); B. Grzadkowski, M. Iskrzynski, M. Misiak, and J. Rosiek, JHEP **1010**, 085 (2010).
- [3] J. de Vries, E. Mereghetti, R. G. E. Timmermans, and U. van Kolck, Phys. Rev. Lett. **107**, 091804 (2011).
- [4] F. J. M. Farley *et al.*, Phys. Rev. Lett. **93**, 052001 (2004); Y. F. Orlov, W. M. Morse, and Y. K. Semertzidis, Phys. Rev. Lett. **96**, 214802 (2006); C. J. G. Onderwater, J. Phys. Conf. Ser. **295**, 012008 (2011).
- [5] J. de Vries, R. Higa, C. -P. Liu, E. Mereghetti, I. Stetcu, R. G. E. Timmermans, and U. van Kolck, Phys. Rev. C **84**, 065501 (2011).
- [6] D. B. Kaplan, M. J. Savage, and M. B. Wise, Phys. Lett. B **424** (1998) 390; D. B. Kaplan, M. J. Savage, and M. B. Wise, Nucl. Phys. B **534** (1998) 329.
- [7] S. Fleming, T. Mehen, and I. W. Stewart, Nucl. Phys. A **677** (2000) 313.

- [8] S. R. Beane, P. F. Bedaque, M. J. Savage, and U. van Kolck, Nucl. Phys. A **700**, 377 (2002); A. Nogga, R. G. E. Timmermans, and U. van Kolck, Phys. Rev. C **72**, 054006 (2005).
- [9] I. B. Khriplovich and R. V. Korkin, Nucl. Phys. A **665**, 365 (2000).
- [10] C.-P. Liu and R. G. E. Timmermans, Phys. Rev. C **70**, 055501 (2004).
- [11] C.-P. Liu and R. G. E. Timmermans, Phys. Lett. B **634**, 488 (2006).
- [12] R. B. Wiringa, V. G. J. Stoks, and R. Schiavilla, Phys. Rev. C **51**, 38 (1995).
- [13] V. G. J. Stoks, R. A. M. Klomp, C. P. F. Terheggen, and J. J. de Swart, Phys. Rev. C **49**, 2950 (1994).
- [14] V. Bernard, N. Kaiser, and U.-G. Meißner, Int. J. Mod. Phys. E **4**, 193 (1995).
- [15] E. Mereghetti, W. H. Hockings, and U. van Kolck, Ann. Phys. **325**, 2363 (2010).
- [16] J. de Vries, E. Mereghetti, R. G. E. Timmermans, and U. van Kolck, in preparation.
- [17] J. de Vries, E. Mereghetti, R. G. E. Timmermans, and U. van Kolck, Phys. Lett. B **695**, 268 (2011).
- [18] S. Kolling, E. Epelbaum, H. Krebs, and U.-G. Meißner, Phys. Rev. C **84**, 054008 (2011).
- [19] C. M. Maekawa, E. Mereghetti, J. de Vries, and U. van Kolck, Nucl. Phys. A **872**, 117 (2011).
- [20] C.-P. Liu, Phys. Rev. C **75**, 065501 (2007).
- [21] J. de Vries, E. Mereghetti, R. G. E. Timmermans, and U. van Kolck, in preparation.
- [22] E. Mereghetti, J. de Vries, W. H. Hockings, C. M. Maekawa, and U. van Kolck, Phys. Lett. B **696**, 97 (2011); K. Ottnad, B. Kubis, U.-G. Meißner, and F.-K. Guo, Phys. Lett. B **687**, 42 (2010).